# Progress in GaAs-Based Metamorphic Technology

W.E. Hoke, C.S. Whelan, P.F. Marsh, P.J Lemonias, P.S. Lyman, S. M. Lardizabal, R.E. Leoni, T.E. Kazior, A. Torabi
Raytheon RF Components, 362 Lowell St., Andover, MA 01810
978-684-8581; whoke@rrfc.raytheon.com

J.-H. Jang, D.C. Dumka, I. Adesida, K.L. Chang, K.C. Hsieh
Dept. of Electrical and Computer Engineering, Microelectronics Laboratory, Univ. of Ill., Urbana, Ill. 61801

## ABSTRACT

**Rapid progress is being made in the application of metamorphic growth technology to various device structures. In this work, the material quality of metamorphic structures grown on GaAs substrates is examined as well as recent results for metamorphic HEMTs, PIN diodes, and HBTs.**

## INTRODUCTION

Currently GaAs devices are fabricated from layer structures that lattice match or are elastically strained (pseudomorphic) to the substrate. The requirement of close lattice match between substrate and film significantly restricts the possible layer compositions. However, metamorphic device structures have recently been grown on GaAs substrates with very encouraging results. These structures contain a compositionally graded (metamorphic) buffer layer to expand the lattice constant. In transforming the lattice constant, crystalline defects are intentionally formed that are predominantly confined to the metamorphic buffer layer. Nearly dislocation-free device layers with compositions not accessible by pseudomorphic growth on GaAs substrates are then grown on top of the metamorphic buffer layer.

One general application of metamorphic technology is the growth of InP-based structures on GaAs substrates that are available in a larger diameter and are less expensive than InP substrates. Currently a 6-inch GaAs substrate costs approximately $450 compared to more than $1000 for a 4-inch InP substrate. Also InP substrates cleave easier than GaAs substrates leading to increased wafer breakage. This problem is exacerbated with increasing wafer diameter as well as processing requiring wafer thinning such as via holes.

A second application of metamorphic growth is to grade the buffer layer to an arbitrary lattice constant. Consequently new device structures can be achieved which contain layer compositions not accessible on either GaAs or InP substrates due to elastic strain constraints.

## METAMORPHIC MATERIAL PROPERTIES

The metamorphic material was grown on GaAs substrates using a linear indium-graded buffer layer to expand the lattice constant.[1] Antimony has also been used for metamorphic grading.[2] The bottom transmission electron microscope (TEM) micrograph in Figure 1 of the metamorphic buffer layer shows a dense dislocation network that is necessarily formed during the grading to expand the lattice constant. The dislocations are predominantly contained in the metamorphic buffer layer. However, the subsequently grown metamorphic HEMT (MHEMT) device layers in the top micrograph in Figure 1 do not exhibit dislocations and have flat, planar interfaces. From plan view TEM, the dislocation density in the device layers is $\leq 1x10^6$ $cm^{-2}$.[3]

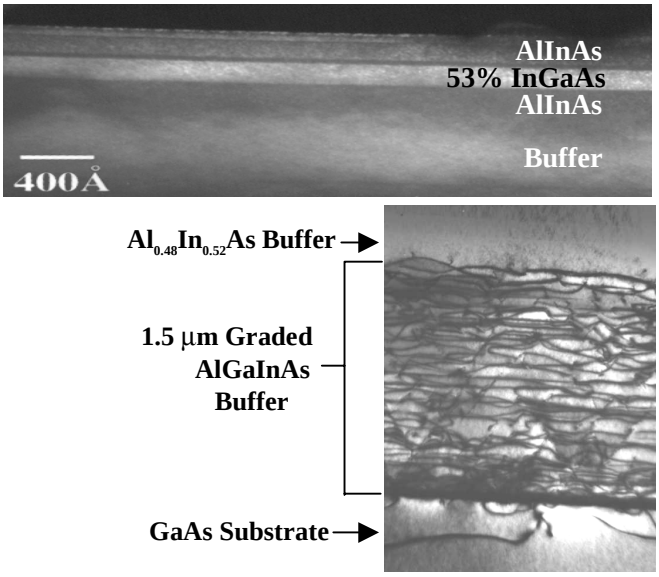


Fig. 1. Cross sectional TEM micrographs of a metamorphic buffer layer (bottom) and MHEMT device layers (top).

The metamorphic surface exhibits a characteristic cross hatch pattern. Surface roughness of metamorphic structures has been examined by atomic force microscopy.[3,4] A typical rms roughness is 10Å, which is considerably smaller than the thinnest critical layers in most device structures.

The optical quality of metamorphic structures has been examined by room temperature photoluminescence (PL) of

the InGaAs channel quantumwell in MHEMT structures. Figure 2 displays the PL spectra of a PHEMT, which has no metamorphic grading defects, and three MHEMTs with increasing indium content. The measurements were taken with the same excitation power density and the spectra were corrected for the detector sensitivity as a function of wavelength. The PL intensities of the MHEMT structures are just as strong as the PHEMT, indicating that nonradiative recombination from metamorphic defects is not quenching the photoluminescence. Figure 2 also illustrates the degree of freedom in grading to arbitrary indium concentrations. (MHEMTs with indium contents higher than 53% have been grown but are not shown in Figure 2 since the optical detector cuts off at longer wavelengths.)

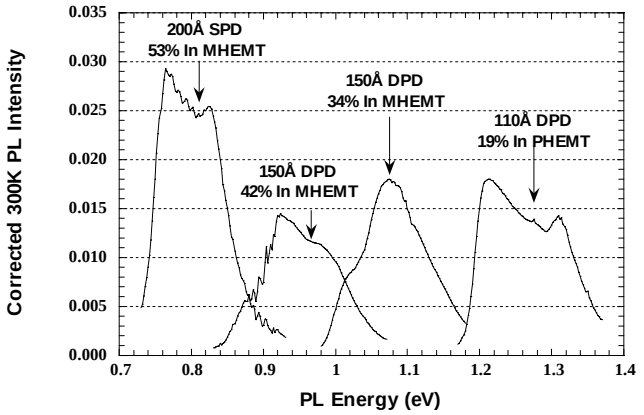


Fig. 2. 300K photoluminescence (PL) from the InGaAs channel layer in a PHEMT and three MHEMT structures. The thicknesses and indium contents of the channel layers are given for SPD (single pulse doped) and DPD (double pulse doped) structures of similar sheet densities (3.2-3.6x$10^{12}$ $cm^{-2}$).

The effect of metamorphic growth on electrical properties has been examined by measuring the transport properties in MHEMT structures. Figure 3 displays room temperature Hall mobilities as a function of indium concentration for a 20% InGaAs channel PHEMT, 5 MHEMT samples, and 2 InP HEMT samples. The expected improvement in mobility with increasing indium concentration in the MHEMT samples is obtained. The 34% In MHEMT mobility is measurably higher than the 20% InGaAs PHEMT which has no metamorphic defects. The two InP HEMT samples have the same single pulse doped structure as the corresponding two MHEMT samples. The mobilities are nearly the same as well as the channel sheet densities (3.3x$10^{12}$ $cm^{-2}$).[1]

## METAMORPHIC DEVICE RESULTS

The MHEMT analog of the InP HEMT is the most developed metamorphic GaAs device structure. The high indium content of the InGaAs channel enables high frequency, low noise performance. Microwave measurements on an MHEMT with a 0.13 μm gate and $In_{0.53}Ga_{0.47}As$ channel layer yielded an extrapolated peak $F_t$ and $F_{max}$ of 235 GHz and 210 GHz, respectively.[5] The high gain and low noise performance of a 3-stage MHEMT LNA is illustrated in Figure 4.[6] The channel layer was $In_{0.60}Ga_{0.40}As$. A noise figure of 1.5 dB and associated gain of 23 dB were obtained from 31-32 GHz. The circuit consumed only 15 mW of total DC power which is particularly attractive for satellite applications.

The high indium content MHEMT is also attractive for wideband, highly linear LNA circuits. The high gain can be traded off for bandwidth. Also the deep channel well reduces parallel conduction in the barrier layers, improving the linearity of the circuit. Figure 5 displays the performance of a 3-stage 1-5 GHz wideband LNA. An $In_{0.60}Ga_{0.40}As$ channel layer was incorporated in the structure. Across a factor of 5 in bandwidth, the circuit exhibited a noise figure of 1.4 dB with a linearity third order intercept of approximately 30 dBm. The circuit also exhibited more than 35 dB of gain and dissipated only 395 mW of DC power. Figure 5 also displays results obtained elsewhere for GaAs PHEMT circuits with similar peripheries. The MHEMT performance compares favorably with these results.

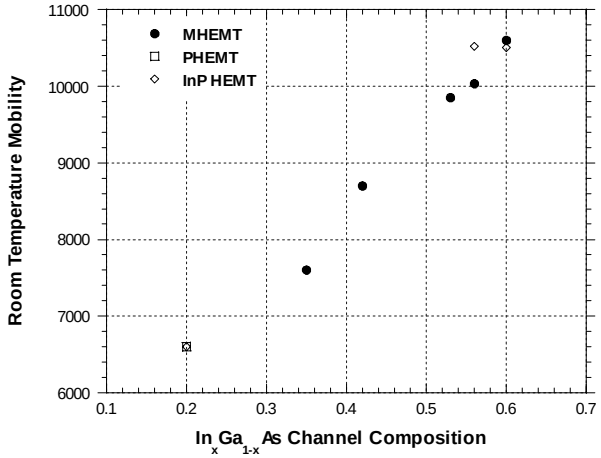


Fig. 3. Room temperature mobility as a function of indium concentration in the InGaAs channel layer for PHEMT, MHEMT, and InP HEMT structures.

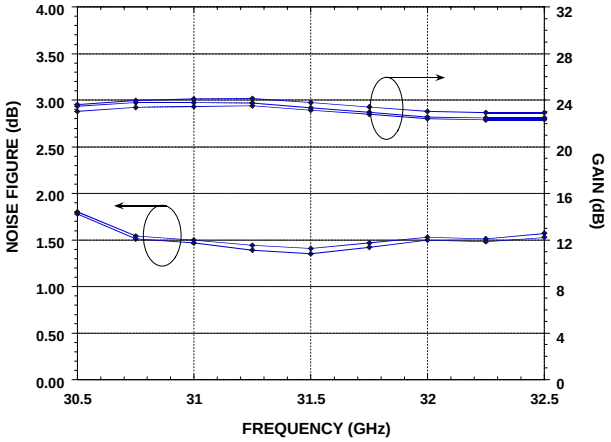

Fig. 4. Noise figure and gain at 31-32 GHz for a 3-stage LNA MHEMT amplifier.

The power performance of InP HEMTs and MHEMTs with ≥ 50% indium content is limited by the breakdown of the InGaAs channel layer. Typical on-state breakdowns are only 3-4 volts. An example of the degree of freedom in layer design enabled by metamorphic growth is the power MHEMT which contains 30-40% indium content in the channel *and* barrier layers. This composition is attractive for increasing the breakdown voltage of the InGaAs channel layer while maintaining much of the high gain, high frequency, low noise performance of the InP HEMT. Furthermore the conduction band discontinuity for charge transfer between the barrier layers and InGaAs channel layer is greater at this indium composition than in GaAs PHEMTs and InP HEMTs.[7] This structure cannot be obtained by pseudomorphic growth on either GaAs or InP substrates due to combined strain from the barrier and channel layers.

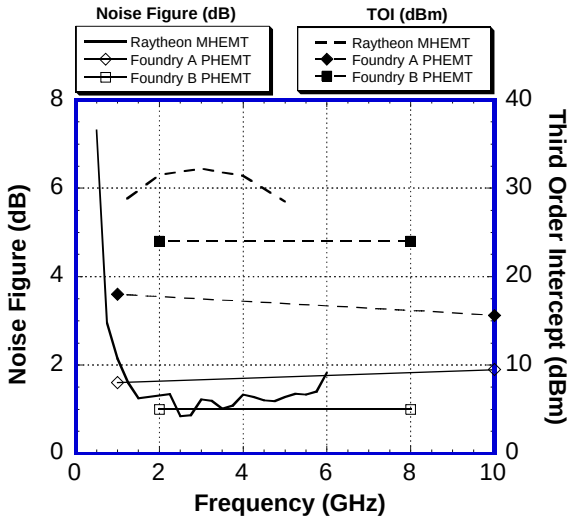


Fig. 5. Noise figure and third order intercept for a 3-stage 1-5 GHz MHEMT amplifier. Results obtained elsewhere for GaAs PHEMTs of similar periphery are also plotted. The MHEMT circuit gain was ≥ 35 dB.

Figure 6 compares power density results (gate widths greater than 250 μm) for MHEMT devices versus the best InP HEMT results for power.[8] Most of the InP HEMT results used a composite InGaAs/InP channel layer to increase the breakdown voltage. A trend line is shown for the InP HEMT results. At 35 GHz, the MHEMT devices exhibit a clear improvement. A power density of 920 mW/mm was produced by an MHEMT with an $In_{0.42}Ga_{0.58}As$ channel layer.

The MHEMT is a majority carrier device. Metamorphic growth has also been applied to the non-majority carrier HBT and PIN diode device structures.[9] The same N-P-N structure was grown metamorphically on a GaAs substrate and lattice matched ($In_{0.53}Ga_{0.47}As$, $In_{0.52}Al_{0.48}As$ compositions) on an InP substrate for baseline comparison. The device layers consisted of: $N^+$ InGaAs/InAlAs contact (1000Å/500Å, $1x10^{19}$ $cm^{-3}$), N InAlAs emitter (1500Å, $6x10^{17}$ $cm^{-3}$), InGaAs spacer (100Å), InGaAs $P^+$ base (750Å, $4x10^{19}$ $cm^{-3}$), N InGaAs collector (5000Å, $3x10^{16}$ $cm^{-3}$), and InGaAs subcollector (5000Å, $1x10^{19}$ $cm^{-3}$). The base doping was achieved with beryllium. Despite the high base doping, SIMS measurements showed negligible diffusion or surface segregation of beryllium grown on a metamorphic buffer layer.[9]

Large HBT devices were fabricated with 40 μm x 80 μm emitters. Consequently the DC current gain was limited by bulk recombination processes such as from metamorphic defects and not from surface recombination. The forward biased ideality factors for the metamorphic HBT and InP HBT junctions were, respectively, 1.39 and 1.42 for the base-emitter junction and 1.27 and 1.11 for the base–collector junction. Figure 7 displays the transistor curves for the collector current versus collector voltage for metamorphic and InP devices. In the traces, the same scales are used and the base current is increased in 200 μA/steps giving a current gain of 25/division. The I-V curves are quite similar with the MHEMT current gain being 80% of the InP current gain.

Figure 8 displays the Gummel plot of the metamorphic HBT device. The maximum current gain (Ic/Ib) was 30. Optimization of growth conditions and the metamorphic buffer layer should further improve the current gain performance of these preliminary metamorphic devices. It should also be noted that the base and collector currents do not cross at low current values in Figure 8 which can occur due to defects or traps. Ito et. al. have determined that dislocation densities greater than $10^7$ $cm^{-2}$ reduce the current gain in AlGaAs/GaAs HBTs.[10] This defect density is qualitatively consistent with our above results of $10^6$ $cm^{-2}$.

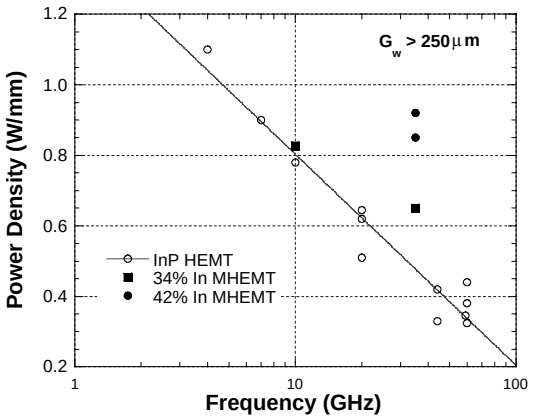


Fig. 6. Power density as a function of frequency for InP HEMTs and MHEMTs with gate widths greater than 250 μm. The trend line is for InP HEMTs.

Metamorphic PIN structures for 1.55 μm operation have also been grown.[9] The active layers consisted of 1000Å

InGaAs $P^+$ contact/1.0 μm undoped InGaAs absorption layer/2000Å InAlAs $N^+$ contact. The same device layers were also grown lattice matched to InP substrates to establish a baseline. As shown in Fig. 9, the responsivity (0.31A/W) of the metamorphic PIN is essentially equivalent to the InP PIN.[11] The responsivities for 50 μm and 100 μm diameter metamorphic PIN diodes (permitting full focusing of the optical radiation on the detector area) was 0.55 A/W, corresponding to an external quantum efficiency of 44%. The metamorphic PIN does have higher dark current (although small, approximately 1 nanoamp in Fig. 9) than the InP PIN. The frequency responses of metamorphic and InP PINs were also measured and found to also be essentially the same.[12] For 20 μm and 25 μm diodes, the bandwidths exceeded the 20 GHz limitation of the test apparatus.

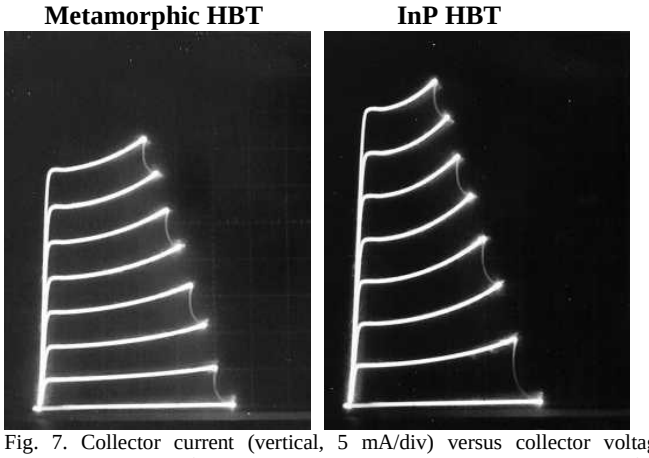


Fig. 7. Collector current (vertical, 5 mA/div) versus collector voltage (horizontal, 1V/div.) for metamorphic and InP HBTs with emitter area of 40 μm x 80 μm. The base current was increased in 200 μA/steps giving a current gain of 25/div.

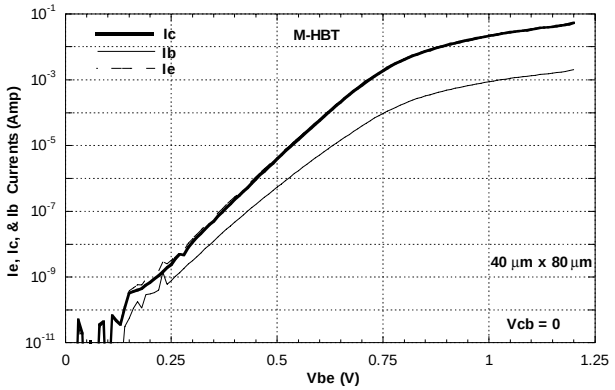


Fig. 8. Gummel plot for a metamorphic HBT with emitter size of 40 μm x 80 μm. Ic, Ib, and Ie are the collector, base, and emitter currents. Vbe is the base-emitter voltage.

## SUMMARY

Excellent MHEMT device and circuit results have been obtained for gain, noise figure, linearity, bandwidth, and frequency performance. In test comparisons, metamorphic material and devices (HEMT, HBT, PIN diode) exhibited similar performances to conventional InP material and devices. Metamorphic growth of high power density MHEMT devices, with structures not accessible on either GaAs or InP substrates, has also been demonstrated.

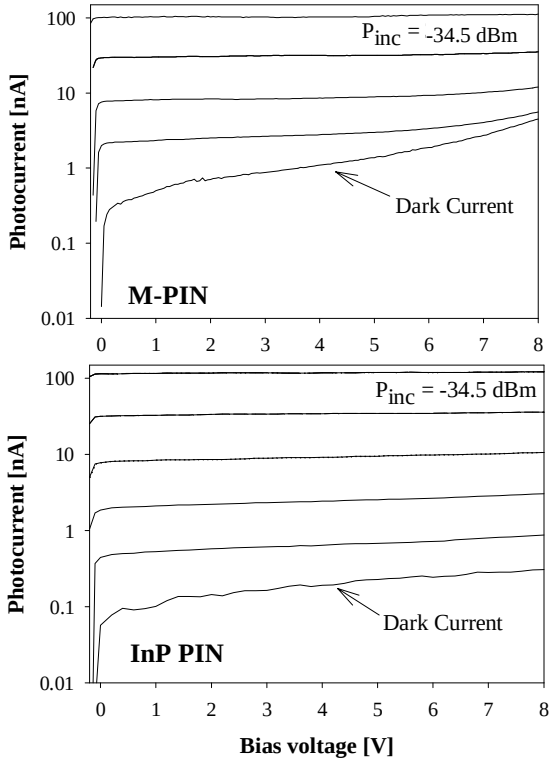


Fig. 9. DC photoresponse to 1.55 μm laser illumination for 25 μm metamorphic and InP PIN devices. The family of curves was generated by reducing the incident radiation (-34.5 dBm) in 6 dB steps.

## REFERENCES

1. W.E. Hoke, P.J. Lemonias, J.J. Mosca, P.S. Lyman, A. Torabi, P.F. Marsh, R.A. McTaggart, S.M. Lardizabal, and K. Hetzler, J. Vac. Sci. Technol. B **17**, 1131 (1999).
2. K.C. Hwang, P.C. Chao, C. Creamer, K.B. Nichols, S. Wang, D. Tu, W. Kong, D. Dugas, and G. Patton, IEEE Electron Device Lett. **20**, 551 (1999).
3. W.E. Hoke, P.J. Lemonias, T.D. Kennedy, A. Torabi, E.K. Tong, K.L. Chang, and K.C. Hsieh, submitted to J. Vac. Sci. Techol. B.
4. W.E. Hoke, P.S. Lyman, C.S. Whelan, J.J. Mosca, A. Torabi, K.L. Chang, and K.C. Hsieh, J. Vac. Sci. Technol. B **18**, 1638 (2000).
5. D.C. Dumka, G. Cueva, W.E. Hoke, P.J. Lemonias, and I. Adesida, Proc. 58th Device Research Conf., Denver, 2000, pp 83-84.
6. P.F. Marsh, S. Kang, R. Wohlert, P.M. McIntosh, W.E. Hoke, R.A. McTaggart, S.M. Lardizabal, R.E. Leoni III, C.S. Whelan, P.J. Lemonias, and T.E. Kazior, 1999 GaAs IC Symposium, pp 225-228.
7. C.S. Whelan, W.E. Hoke, R.A. McTaggart, S.M. Lardizabal, P.S. Lyman, P.F. Marsh, and T.E. Kazior, IEEE Electron Device Lett. **21**, 5 (2000).
8. C.S. Whelan, P.F. Marsh, S.M. Lardizabal, W.E. Hoke, R.A. McTaggart, and T.E. Kazior, Proc. GaAs and Other Semiconductor Applications Symposium, Paris, 2000, pp. 189-192.
9. W.E. Hoke, P.J. Lemonias, T.D. Kennedy, A. Torabi, E.K. Tong, R.J. Bourque, J.-H. Jang, G. Cueva, D.C. Dumka, I. Adesida, K.L. Chang, and K.C. Hsieh, submitted to J. Vac. Sci. Technol. B.

10. H. Ito, O. Nakajima, T. Furuta, and J.S. Harris, IEEE Elect. Dev. Lett. **13**, 232 (1992).
11. J.H. Jang, G. Cueva, D.C. Dumka, W.E. Hoke, P.J. Lemonias, and I. Adesida, Proc. 58th Device Research Conf., Denver, June 19-21, 2000, pp. 173-174.
12. J.H. Jang, G. Cueva, D.C. Dumka, W.E. Hoke, P.J. Lemonias, and I. Adesida, accepted to Photonics Tech. Lett., 2001.